Experimental and Theoretical Analysis of the Interaction of (±)-*cis*-Ketoconazole with β-Cyclodextrin in the Presence of (+)-L-Tartaric Acid

ENRICO REDENTI,*,† PAOLO VENTURA,† GIOVANNI FRONZA,‡ ANTONIO SELVA,‡ SILVIA RIVARA,§ PIER VINCENZO PLAZZI,§ AND MARCO MOR§

Contribution from *Chemical and Biopharmaceutical Department, Chiesi Farmaceutici S.p.A., Via Palermo, 26/A, I-43100 Parma, Italy, Centro di Studio del CNR sulle Sostanze Organiche Naturali, Dipartimento di Chimica, Politecnico di Milano, Via Mancinelli 7, I-20131 Milano, Italy, and Dipartimento Farmaceutico, Università degli Studi di Parma, Viale delle Scienze, I-43100 Parma, Italy.*

Received December 7, 1998. Accepted for publication March 17, 1999.

Abstract □ ^{1}H NMR spectroscopy was used for determining the optical purity of *cis*-ketoconazole enantiomers obtained by fractional crystallization. The chiral analysis was carried out using β-cyclodextrin in the presence of (+)-L-tartaric acid. The mechanism of the chiral discrimination process, the stability of the complexes formed, and their structure in aqueous solution were also investigated by ^{1}H and ^{13}C chemical shift analysis, two-dimensional NOE experiments, relaxation time measurements, and mass spectrometry experiments. Theoretical models of the three-component interaction were built up on the basis of the available NMR data, by performing a conformational analysis on the relevant fragments on ketoconazole and docking studies on the components of the complex. The model derived from a folded conformation of ketoconazole turned out to be fully consistent with the molecular assembly found in aqueous solution, as inferred from NOE experiments. An explanation of the different association constants for the complexes of the two enantiomers is also provided on the basis of the interaction energies.

Introduction

Ketoconazole, 1-acetyl-4-[4-[[2-(2,4−dichlorophenyl)-2-(1*H*-imidazol-1-yl-methyl)-1,3-dioxolan-4-yl]methoxy]phenyl]piperazine, is a potent, orally active broad-spectrum antifungal agent[1,2] which is marketed as a racemic mixture of the *cis*-(2*S*,4*R*) and -(2*R*,4*S*) enantiomers.

The (−)-stereoisomer is (2*S*,4*R*).[3] Both the enantiomers of ketoconazole (KC) were stereoselectively prepared,[3,4] as it has been claimed that the optically pure compounds are more effective than the racemic one for treating local and systemic fungal infections in humans.[5] One of the current active research areas in host−guest or supramolecular chemistry is chiral recognition by cyclodextrins (CDs). Both naturally occurring (α, β, and γ) and derivatized CDs are indeed extensively used in chromatography (bonded to the stationary phase or in the eluate) for the separation of enantiomers[6] and as chiral shift reagents for NMR determination of enantiomeric composition.[7,8] In this paper we report a ^{1}H NMR method for determining the optical purity of the ketoconazole enantiomers obtained by fractional crystallization. Chiral analysis was carried out using β-cyclodextrin (βCD) in the presence of (+)-L-tartaric acid (hereafter TA), as it has been found that simultaneous inclusion and salt formation yield complexes freely soluble in water. For instance, KC solubility is enhanced by several orders of magnitude, while that of βCD increases by more than 10 times.[9−13] The stability of the complexes formed and their structure in aqueous solution were investigated by NMR spectroscopy and ionspray tandem mass spectrometry.[14] In addition, a model of the KC:TA:βCD complex was built up by computational techniques, on the basis of the available NMR data, with the aim of elucidating the chiral discrimination process. Among the different conformations of KC, only those in accordance with intramolecular NOE cross-peaks were selected and submitted to docking studies. The intermolecular distances were measured and related to the intensities of NOE cross-peaks, allowing the selection of a unique interaction pattern. The energies of interaction between the components were calculated for the proposed complexes of both the enantiomers of KC.

Materials and Methods

(±)-*cis*-Ketoconazole was a kind gift from RGR Co. (Milan, Italy).

Samples of (+)-(2*R*,4*S*) (ee ≈ 98%) and (−)-(2*S*,4*R*)-ketoconazole ee ≈ 98%) were obtained from the racemate by fractional crystallization of the diastereomeric salts with (−)- and (+)-10-camphorsulfonic acid, respectively. The corresponding equimolar tartrate salts were prepared by freeze-drying their aqueous solutions. β-cyclodextrin (water content ≈ 10%) and D_2O (99.8%) were purchased from Roquette Co. (Lestrem, France) and from Merck Co. (Milan, Italy), respectively. All other reagents were of analytical grade. Solutions of 10 mM drug concentration and guest-to-host ratio at 1:1.5 were used unless otherwise specified.

NMR spectra were acquired on ACF 200 and ARX 400 spectrometers (Bruker, Karlsruhe, Germany). Chemical shifts were referred to external TSP (sodium, 3-(trimethylsilyl)propionate) at 0 ppm (accurate to ± 0.001 ppm). The phase-sensitive ROESY (Rotating-frame Overhauser Effect SpectroscopY) experiments were performed using a 3.5 kHz spin-lock field and a mixing time of 350 ms. T_1 relaxation time measurements were made using the inversion recovery method. Fifteen different τ delays varying from 0.05 to 10 s between 180° and 90° pulses were used. A regression procedure was used to fit the relaxation data to the exponential equation $M = \mathrm{Mo}(1 - 2e^{-\tau/t})$.

For the determination of the association constants k of the two enantiomers, the concentration of *rac*-ketoconazole tartrate was kept at 1 mM while that of βCD varied between 5 and 20 mM. The change in the chemical shift of the H20 proton, which splits upon βCD addition, was monitored during the titration. The data were evaluated according to the Foster−Fyfe[15] modification of the Benesi−Hildebrand equation:[16]

$$\Delta\delta_{obs}([B]_t)^{-1} = k(\Delta\delta_c - \Delta\delta_{obs})$$

* Corresponding author. Tel: ++39 0521 279662. Fax: ++39 0521 774468.
† Chiesi Farmaceutical S.p.A.
‡ Centro di Studio del CNR sulle Sostanze Organiche Naturali.
§ Università degli Studi di Parma.

10.1021/js980468o CCC: $18.00
Published on Web 04/24/1999

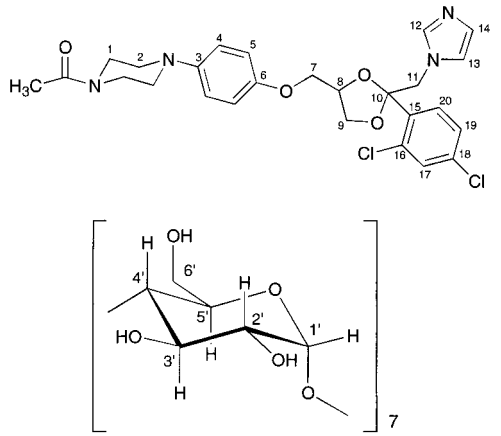

Figure 1—Hydrogen-labeling scheme for KC and βCD.

where $[B]_t$ is the total concentration of host, $\Delta\delta_{obs}$ is the difference between the chemical shift observed and the chemical shift of the free guest for a given proton, and $\Delta\delta c$ is the chemical shift difference (for a given proton) between the free guest and the pure complex.

The statistical analysis was performed by using SAS program version 3.1 (SAS Institute Inc., Cary, NC).

The mass spectra were acquired on a benchtop API 300 triple quadrupole mass spectrometer (Perkin-Elmer, Norwalk, CT), equipped with a standard API−Ionspray ionization source. Tandem MS experiments were carried out operating with a collision energy (E_{lab}) of 30 eV, using nitrogen as collision gas at a pressure of 8 mTorr. The 1:1:1 (+)-KC:TA:βCD and (−)-KC:TA:βCD samples were dissolved in 50/50 (v/v) water/acetonitrile and diluted to a concentration of 1000 ppm. The tandem MS analysis was repeated six times for each sample.

Molecular modeling studies were performed with the Sybyl 6.3 Software (Tripos Inc., 1699 South Hanley Rd., St. Louis, MO, 63144), running on a Silicon Graphics R4400 (200 MHz 64 Mb RAM) Indigo2 workstation. Three-dimensional models of (+)-TA and *cis*-KC were built and energy-minimized using the standard Tripos force field, with the Powell minimization method[17] and a convergence gradient of 0.05 kcal/mol·Å. The minimum-energy geometry of *cis*-(2*R*,4*S*)-KC was in good agreement with the crystal structure reported in Cambridge Structural Database (CSD) (ref code: KCONAZ),[18] with the exception of the torsion angle between the benzene and the piperazine rings; in fact, they lie on the same plane in the crystal structure and are perpendicular in the minimum-energy conformation obtained with Tripos force field. βCD structure was taken from CSD (ref code: BCDEXD10),[19] deleting the cocrystallized water molecules, and its geometry was kept fixed. Charges were calculated using the Gasteiger−Hückel method, giving an initial formal charge of +1 to the N^3 atom of the imidazole ring of KC and of −0.5 to the two O atoms of one of the carboxylic groups of TA, to simulate the same conditions of ionization as supplied in NMR studies (pH = 3.5); the dielectric function was dependent on 1/*r*.

A systematic conformational analysis on KC, with rotation of bonds C10−C11, C8−C7, C7−O with steps of 120°, and of O−C6 (Figure 1) with two steps of 90° (that is, with C7−O coplanar and perpendicular to the phenoxy ring), was performed in order to generate the possible KC conformations and was followed by energy minimization (with electrostatic term ignored). The orientations of the imidazole and the dichlorophenyl rings were not changed, nor were all possible conformations of the dioxolane and acetylpiperazine rings created (see Results and Discussion for a comment). Only those conformations having H−H distances lower than 3.5 Å for couples of protons giving high-intensity NOE cross-peaks were selected for subsequent docking studies.

Docking was performed with the DOCK routine of Sybyl, in a region of space including the three components of the complex, with a 0.5 Å grid resolution. Docking between KC (considered as the ligand in the docking routine) and βCD (considered as the site) was based on steric interaction energy only; the electrostatic contribution was considered for the subsequent docking of TA (ligand) onto the KC:βCD complex (site); during the docking procedure, the geometry of the site was kept fixed. Inter- and intramolecular distances were measured after energy minimization of the whole complex, with fixed geometry of the βCD ring (considered as an aggregate in Sybyl); for equivalent hydrogens, the minimum distance was chosen. βCD was eventually rotated around the axis connecting C15 and C18 of KC with steps of 30°, and the 12 resulting models were energy-minimized as reported.

MOLCAD[20] was used for the representation of the lipophilicity potential at the solvent accessible surface of KC and βCD.

Results and Discussion

NMR Studies—The formula of ketoconazole in Figure 1 shows the numbering system employed, which is different from the IUPAC notation. The spectral features of its tartrate salt in the absence and in the presence of βCD in 1.5 molar ratio are given in Table 1 and Table 2. An excess of the host was used in order to improve the separation between the pair of signals of the two enantiomers of the drug.

The difference between the enantiomers in the bound state and the free state ($\Delta\delta$) and the difference between the two bound states ($|\Delta\Delta\delta|$) are given in frequency units (Hz) rather than ppm, as, in this way, small changes can be better appreciated. In the ^{1}H NMR spectrum of (±)-*cis*-ketoconazole tartrate, on addition of βCD, two sets of resonances are observed for most of the protons or groups of equivalent protons, indicating that inclusion complex formation with βCD induces nonequivalence in the proton nuclei of the two enantiomers of the drug. As far as βCD is concerned, the ^{1}H resonances of the inner protons H3′ and H5′ show the diagnostic upfield shift due to the inclusion of the aromatic ring of the guest in the cavity.[21] Among the aromatic resonances, the largest shifts in δ were observed for the protons belonging to the imidazolium moiety, which also show splitting upon inclusion. The protons belonging to the dichlorophenyl moiety, which is the part of the molecule involved in the inclusion complex formation (vide ultra), experience smaller downfield shifts[22] and only the proton H20 shows splitting of the signal as well ($|\Delta\Delta\delta| = 8.8$ Hz). The upfield shift of the alkyl- and H4 aromatic protons may be due to conformational changes produced by the inclusion. Similar changes in the ^{13}C NMR spectra were also observed. Doubling of some of the aromatic resonances was observed, while only the C9 and C7 aliphatic carbons split. Analysis of the complexation-induced ^{13}C chemical shift changes allows some preliminary considerations on the geometry. According to Inoue,[23] the inclusion of the guest molecule into the CD cavity causes upfield shifts of the signals of the included carbons and downfield displacements of the signals of the carbons externally close to the rims of the truncated cone of CD. The changes observed for the carbons of the dichlorophenyl moiety may suggest that the insertion occurs from the wider rim of the cavity in such a way as to leave the carbons C15 and C18 exposed to the aqueous medium. The downfield shift of the carbon C16 is probably a consequence of the steric interaction[24] between the chlorine atom and the closely spaced hydrogens.

The coupling constants of the single enantiomers of KC were measured to check whether conformational changes were induced upon complexation. Since all values show no difference (Table 1) between the enantiomers, it seems to be the different orientation inside the cavity and/or outer-sphere interaction (intermolecular hydrogen bonds), rather than a different conformation of the enantiomers upon inclusion, that makes chiral discrimination possible. The more evident changes in differential chemical shifts for the signals of the imidazolium moiety in comparison to the signals of the dichlorophenyl moiety directly involved in the inclusion complex formation may indicate that the

Table 1—Tabulation of Coupling Constants (J) and ^{1}H Chemical Shifts (δ), for Free *rac*-Ketoconazole Tartrate and Its Multicomponent Complexes

assignment	J (Hz)	δ (±)-KC:TA	δ (+)-KC:TA:βCD	δ (–)-KC:TA:βCD	$\Delta\delta$ (Hz) (–)	$\Delta\delta$ (Hz) (+)	$\lvert\Delta\Delta\delta\rvert$
CH_3CO		2.186	2.154		–14.4		–
H2 (t)	$^3J = 4.8$	3.254	3.176	3.160	–37.6	–31.2	6.4
H2′ (t)	$^3J = 5.2$	3.314	3.225	3.213	–40.4	–35.6	4.8
H9 (dd)	$^2J = 10.8$ $^3J = 6.3$	3.549	hidden by CD signals				
H1 (t)[a]	$^3J = 7.0$	3.802	hidden by CD signals				
H1′ (t)[a]	$^3J = 6.8$	3.811	hidden by CD signals				
H7 (dd)[b]	$^2J = 8.8$ $^3J = 5.2$	3.859	3.948[c]	3.962[c]	41.2	35.6	5.6
H7′ (dd)[b]	$^2J = 8.8$ $^3J = 7.3$	3.966	4.009	3.933	–13.2	17.2	30.4
H9′ (dd)	$^2J = 10.8$ $^3J = 2.8$	4.064	4.100	4.065	0.4	14.4	14.0
H8 (m)		4.494	4.421	4.489	–2.0	–29.2	27.2
C*H*OH (s)		4.519	4.50		–7.6		–
H11	$^2J = 14.8$	4.913	4.931	4.958	18.0	7.2	11.8
H11′	$^2J = 14.8$	4.817	4.827	4.801	–6.4	4.0	10.4
H5 (d)	$J = 9.1$	6.973	6.940	6.934	–15.6	–13.2	2.4
H4 (d)	$J = 9.1$	7.241	7.121		–48.0		–
H14 (t)	$J = 1.6$	7.289	7.364	7.334	18.0	30.0	12.0
H19 (dd)	$J = 8.5$ $J = 2.1$	7.444	7.517	7.517	29.2		–
H13 (t)	$J = 1.6$	7.482	7.622	7.606	49.6	56.0	6.4
H17 (d)	$J = 2.1$	7.654	7.666		4.8		–
H20 (d)	$J = 8.5$	7.712	7.784	7.805	37.2	28.8	8.4
H12 (t)	$J = 1.6$	8.747	8.884	8.868	48.4	54.8	6.4

[a,b] Assignments may be interchanged. [c] ABX system

Table 2—Tabulation of ^{13}C Chemical Shifts (δ)

assignment	δ (±)-KC:TA	δ (+)-KC:TA:βCD	δ (–)-KC:TA:βCD	$\Delta\delta$ (+)	$\Delta\delta$ (–)	$\lvert\Delta\Delta\delta\rvert$
CH_3CO	22.711	22.652		–3.0		–
C1′	42.807	43.580		38.9		–
C1	47.396	48.253		43.1		–
C2	54.697	53.758		–47.3		–
C2′	55.030	54.710		–16.1		–
C11	55.220	54.828		–19.7		–
C9	68.371	68.455	68.800	4.2	21.6	17.4
C7	70.797	70.489	70.310	–15.5	–24.5	9.0
CHOH	75.031	75.233		10.2		–
C8	77.171	77.599		21.5		–
C10	109.609	109.395		–10.8		–
C5	118.527	118.551	118.504	1.2	–1.2	2.4
C13	121.238	121.310		3.6		–
C4	123.473	122.282		–59.9		–
C14	126.375	126.696		16.2		–
C19	130.013	129.491		–26.3		–
C20	132.487	132.285	132.178	–10.2	–15.5	5.3
C17	133.676	133.224		–22.7		–
C15	134.841	135.424	135.543	29.3	35.3	6.0
C16	135.102	135.876		39.0		–
C18	138.456	138.718	138.742	13.2	14.4	1.2
C12	138.622	139.027	139.075	20.4	22.8	2.4
C3	142.380	145.698	145.793	167.0	171.8	4.8
C6	158.456	156.875	156.792	–79.6	–83.7	4.1
CH_3CO	175.055	174.426		–31.7		–
COOH	178.242	178.659		21.0		–

strength of the "outer-sphere" interactions between the nitrogen atoms and the secondary hydroxyl groups probably plays the main role in the chiral discrimination process. For most of the signals, both the shielding and deshielding are more pronounced for the (–)-KC:TA:βCD complex than for the (+)-KC:TA:βCD complex, suggesting a stronger intermolecular interaction for the former enantiomer.

The H14 signal has the greatest potential for optical purity determination. It occurs as a pair of well-resolved narrow triplets (J = 1.6 Hz) of 12 Hz separation at 400 MHz, allowing the most accurate integration of each signal. Larger splitting in substrate resonance can be observed (e.g., H8 gives rise to a pair of well-resolved multiplet – $|\Delta\Delta\delta|$ = 27 Hz), but no attempts were made to determine the optical purity from these changes. By monitoring the H14 signal at 400 MHz, the resolved (–)-enantiomer turned out to contain about 2% of isomeric impurity (see Figure 2). The results we obtained would suggest that 1% optical purity measurements could be attainable by this method.

To further explore differences in these weakly bound diastereomeric complexes, T_1 measurements were made on free (±)-*cis*-ketoconazole tartrate and its βCD complex. The results are presented in Table 3. Only the protons for which it was possible to determine the T_1 values with sufficient accuracy (no overlapping with other signals) are reported. In general, the T_1 values for KC protons reduce in the presence of βCD in accordance with the fact that the correlation time of the guest increases upon complex formation. In particular, a dramatic reduction was observed for proton H17, which relaxes very slowly as it lacks nearby protons. Among the resonances which split, T_1 reduces more for protons H14 and H13 of the (–)-enantiomer; this difference in reduction may once again be attributed to a tighter binding of this enantiomer.

In the case of proton H20, both (–)- and (+)-form display equal reduction in T_1, confirming that the orientation of the dichlorophenyl ring inside the cavity is probably very similar for the two enantiomers. T_1 of the tartrate protons also reduces dramatically, suggesting that the counterion is strictly involved in the molecular assembly. Since complexes stability is important in determining chiral discrimination, a correlation was sought with the findings reported above, i.e., larger differences in shift and in T_1 reduction for the (–)-enantiomer. The two enantiomers of (±)-ketoconazole form 1:1 inclusion complexes as they possess only one binding site, i.e., the dichlorophenyl ring. The consistency of the stoichiometric model with the solubility diagram has also been reported in the litera-

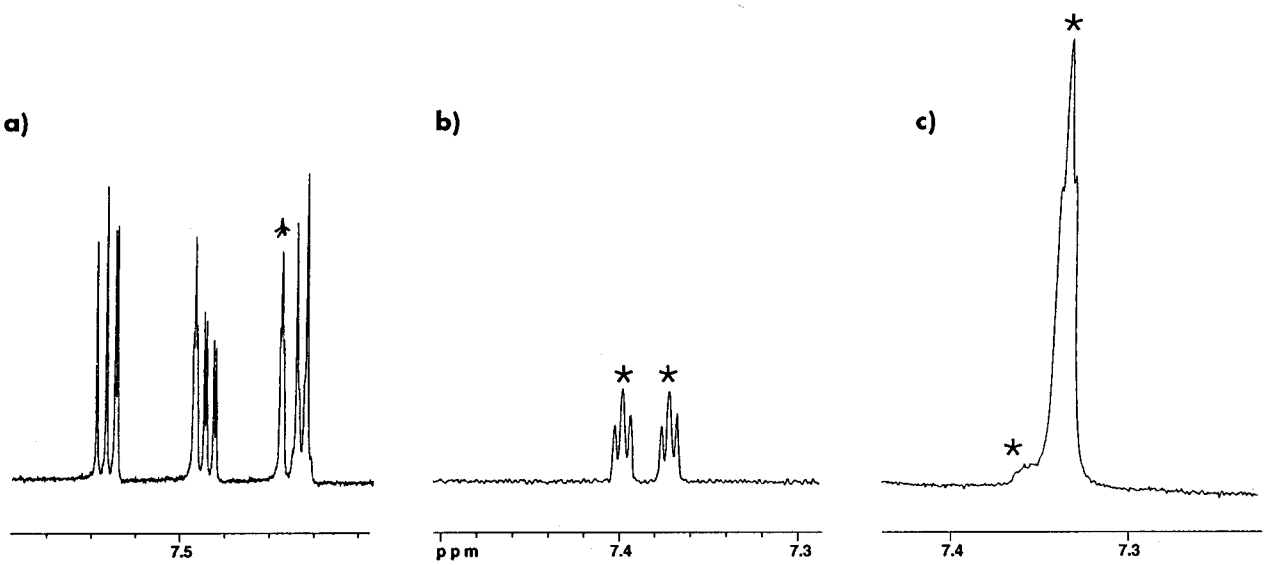

Figure 2—400 MHz H14 signal (*) of (a) (±)-KC:TA 1:1; (b) (±)-KC:TA:βCD 1:1:1.5; (c) (–)-KC:TA:βCD (ee = 98%).

Table 3—Tabulation of T_1 Values (s) for Some ^{1}H Resonances

assign-ment	T_1 (±)-KC:TA	T_1 (+)-KC:TA:βCD	T_1 (–)-KC:TA:βCD	ΔT_1 (+)	ΔT_1 (–)	$\lvert\Delta\Delta T_1\rvert$
H12	2.20	0.89	0.87	–1.31	–1.33	0.02
H20	1.18	0.30	0.30	–0.88		–
H17	10.76	0.60		–10.16		–
H13	1.78	0.83	0.61	–0.95	–1.17	0.22
H19	1.90	0.48		–1.42		–
H14	2.55	1.38	1.31	–1.17	–1.24	0.07
H4	0.70	0.37		–0.33		–
H5	0.77	0.46		–0.31		–
CH (tartrate)	5.70	1.83		–3.87		–
H2	0.46	0.23		–0.23		–
CH_3CO	0.95	0.64		–0.31		–

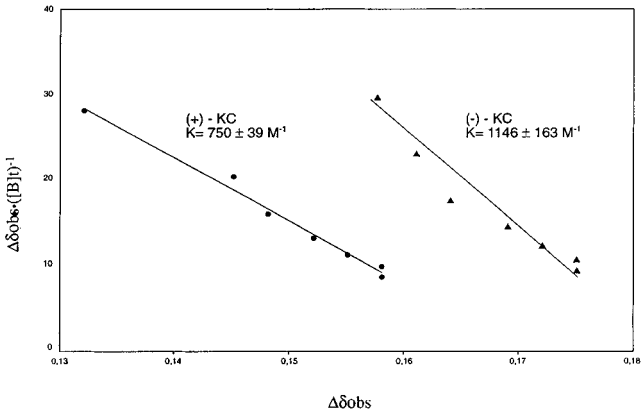

Figure 3—Change in the chemical shift of the H20 proton: (●) (+)-KC; (▲) (–)-KC.

ture.[12] Therefore, the association constants for the two complexes were evaluated by using the Foster–Fyfe equation (see Materials and Methods). The k at 25 °C, obtained from the slope of the straight lines, resulted as being 750 ± 100 M^{-1} for the (+)-enantiomer and 1146 ± 419 M^{-1} for the (–)-enantiomer (Figure 3). The test for heterogeneity of the slopes was positive, indicating that the difference in the complexes stability is statistically significant.

Finally, the stereochemistry of the two complexes was investigated by means of two-dimensional rotating frame NOE (ROESY) spectroscopy. An expansion of the spectrum of the complex of the (–)-enantiomer is reported in Figure 4. Both the enantiomers gave the same NOE pattern. A set of cross-peaks is observed between the inner protons H3′ and H5′ of βCD and the protons H17, H19, and H20, indicating that the inclusion occurs by accommodation of the dichlorophenyl ring. In addition, significant dipolar contacts are observed between H12, H13 (imidazolium), H4, and H5 (phenolic ring) with the H3′ proton of βCD, suggesting that the inclusion must occur from the wider-diameter side of the truncated cone of βCD. The H4 and H5 protons probably interact with H2′ of βCD as well, reflecting the major mobility of the phenolic ring around the "mouth" of the host. Anyway, an unambiguous interpretation is not possible as the signals H2′ and H5′ of βCD and H9 of KC are overlapped (vide ultra).

Mass Studies—Since some authors have recently drawn attention to the use of mass spectrometry for studying chiral selectivity in the inclusion complex formation,[25,26] the relative strength of the interaction binding of the two enantiomers was investigated by ionspray tandem mass spectrometry (ISMS/MS) experiments.[27] The positive ISMS spectra of the samples (Figure 5) exhibit the protonated 1:1:1 KC:TA:βCD (m/z 1815.5), which, upon collision, dissociate, yielding protonated KC:βCD complex (m/z 1665.6) and protonated KC (m/z 531.2). The ratio between the ion current of the two product ions is significantly higher for the (–)-enantiomer, suggesting that it forms a more stable inclusion complex than the other one in the gaseous phase. These findings are in agreement with the data obtained in aqueous solution (vide supra).

Molecular Modeling Calculations—Molecular modeling proved to be an excellent tool for the study of drug–cyclodextrin interaction.[28] The three components of the title complex, namely βCD, KC, and TA, can assume, in aqueous solution, a number of interconverting conformations and can perform different mutual interactions. For βCD alone, for example, the round-shaped conformation is not a minimum energy one, but can be regarded as the result of a time average in the ns-scale.[29] Given the high number of possible βCD conformations and the absence of a correction for the anomeric effect[29] in the Tripos force field here employed, the internal energy for the βCD molecule was not minimized, and its geometry was kept fixed in one of the crystal conformations reported in CSD.[19]

Although KC is a rather flexible compound, the complexation with βCD should select some of the allowed conformations which, in turn, could be identified by the analysis of the intramolecular NOEs (see Figure 4). Pos-

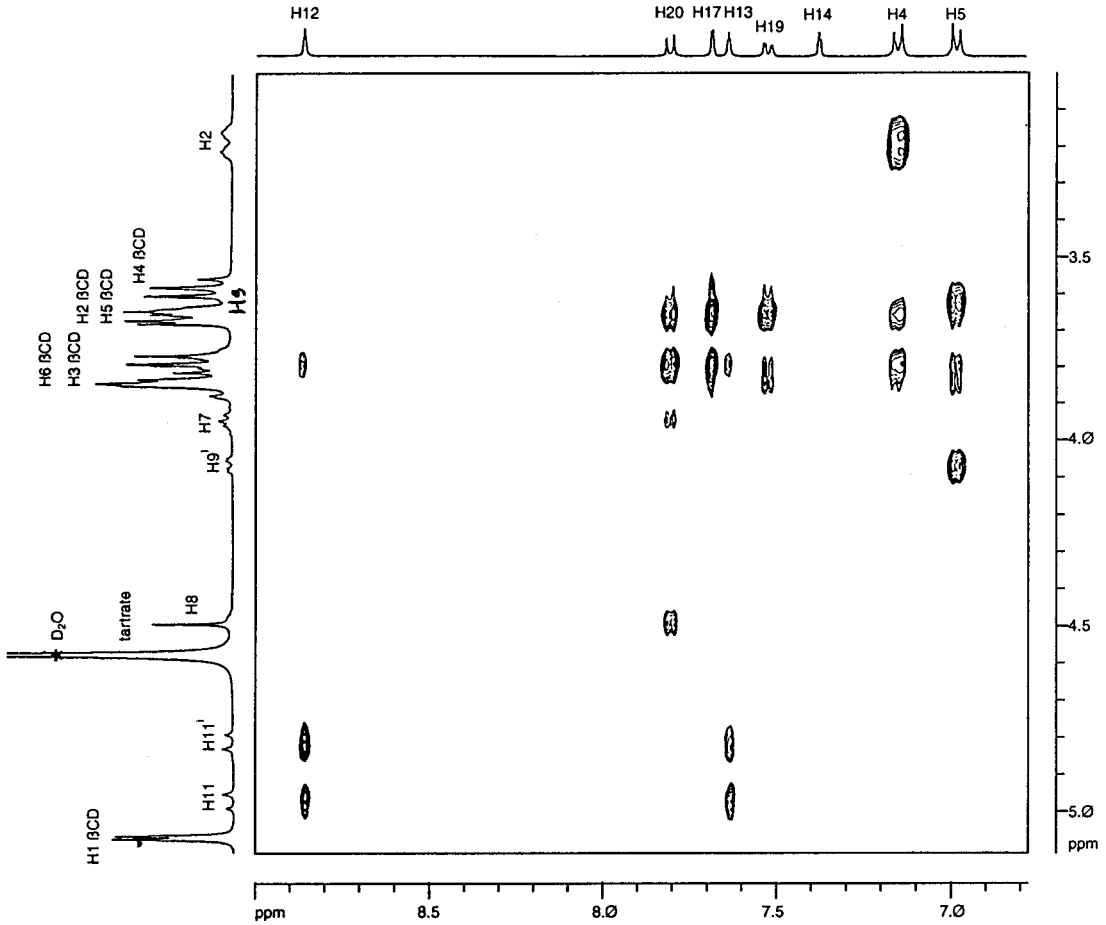

Figure 4—400 MHz ROESY spectrum of (–)-KC:TA:βCD 1:1:1.5.

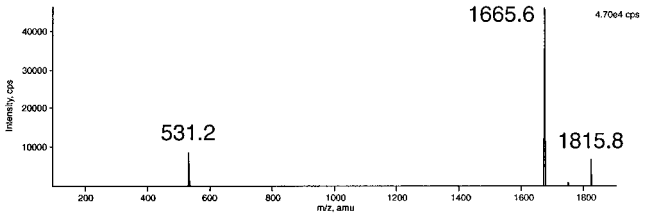

Figure 5—IS MS/MS spectrum of (–)-KC:TA:βCD 1:1:1.

sible conformations were thus chosen on the basis of the cross-peaks between the signals H20−H8, H20−H7, and H5−H9′ (the NMR signal marked as H9′ was assigned to the proton trans to H8). An intramolecular cross-peak between H9 (the dioxolane hydrogen opposite to the side chain) and H5 is also recognizable although it is partly overlapped with the intermolecular cross-peak between H5 and H2′ and/or H5′ of βCD; therefore, the relevant averaged distance was included in the conformation selection criteria. The minimum-energy conformations of KC were generated by rotation of the bonds, causing a variation in the mutual disposition of the fragments showing NOE interactions with βCD, i.e., the dichlorophenyl, the imidazole, and the side-chain phenyl rings. Some preliminary considerations allowed a reduction in the number of conformations to be generated. The dichlorophenyl ring has two possible orientations, with the plane of the ring perpendicular to the C10−C11 bond; the presence of a cross-peak between H20−H8 and H20−H7, but not between H20−H9′, prompted us to consider only the rotamers having H20 pointing toward H8. The imidazole ring is quite free to rotate around C11−N; we kept it in one of the possible orientations because its rotation caused slight variations

Table 4—Torsion Angles (deg) and Intramolecular Distances (Å) for the Conformers of (+)-KC Consistent with NOE Intramolecular Cross-peaks. For the (–)-enantiomer the Intramolecular Distances are the Same, and the Torsion Angles Are Opposite

	1	2	3	4	5	6
			Torsion Angles			
C15C10C11N	60.2	–56.1	178.5	60.7	–55.7	179.3
C9C8C7O	78.7	79.2	78.7	59.2	58.6	57.3
C8C7OC6	–60.4	–60.9	–61.6	56	56	55.2
C7OC6C5	104	103.6	103.7	–110.4	–110.6	–113.5
			Intramolecular Distances			
H20–H8	2.88	2.73	2.77	2.87	2.73	2.75
H20–H7[a]	4.18	4.10	4.13	4.25	4.17	4.20
H5–H9′[b]	3.21	3.23	3.24	2.95	2.88	2.83
H5–H9	3.01	3.01	3.00	2.65	2.68	2.77

[a] Measured from the H7 closer to H20. [b] H9′ is trans to H8.

in the spatial arrangement of the complex, compared to the uncertainty of the model. This means that each generated rotamer is representative of a family of conformations attainable from imidazole rotation. The same applies to the acetylpiperazine moiety, which gave no recognizable NOE interaction with βCD, and whose conformations were not explored. Rotation of the other four single bonds (see Materials and Methods) gave a set of 54 conformations, which were energy-minimized before the calculation of H5−H9 and H5−H9′ distances. Only six conformers, described in Table 4, had these two distances lower than 3.5 Å, and were submitted to docking studies.

While the intramolecular distances between hydrogen atoms of the isolated KC molecule are the same for the corresponding conformers of the two enantiomers (with

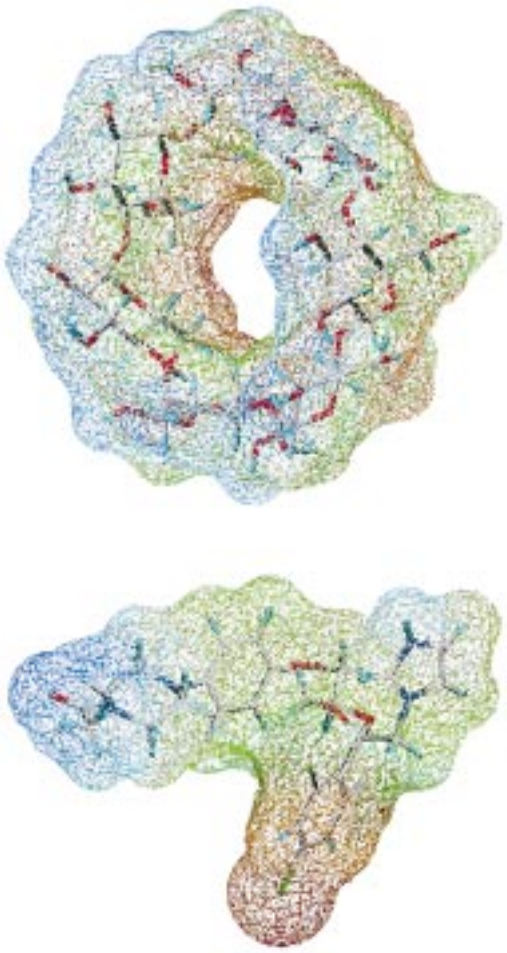

Figure 6—Lipophilicity potential contour maps of βCD, in the crystal structure conformation, and KC in conformation **3** (Table 4), colored according to a lipophilicity scale, ranging from blue (hydrophilic) to brown (lipophilic). Atom color codes – white: carbon; red: oxygen; blue: nitrogen; cyan: hydrogen; green: chlorine.

opposite torsional angles), the complexation with the chiral βCD molecule leads to different interactions for the (+)- and (−)-KC. The docking procedure described as follows was therefore performed on both the KC enantiomers. The analysis of NMR data, in particular NOEs, gives evidence that complexation occurs by involving the dichlorophenyl ring, which is inserted in the βCD cavity from the wider rim (vide supra). This is also supported by the lipophilicity potential of the host and guest molecules at their solvent accessible surface, which is maximum in correspondence to the dichlorophenyl ring and βCD cavity (Figure 6).

Only three (**1**, **2**, and **3**) of the six selected conformations of KC could be docked into the βCD, as the spatial disposition of the side chain, having the phenoxy ring stacked beneath the dichlorophenyl one, prevented the arrangement of βCD around the dichlorophenyl moiety for the other three conformations. The chosen conformations differed from each other only by the imidazolylmethyl group orientation around C10−C11 (Table 4). As a first step, KC was docked into the βCD cavity on the basis of the van der Waals contribution of intermolecular interactions; monoanionic tartrate was then docked onto the KC:βCD complex with the charged carboxylate group involved in a saline bond with the protonated imidazolium ring, and with the uncharged carboxylic group, in gauche conformation, pointing toward the βCD secondary hydroxyl groups, as suggested by the dramatic relaxation time variation of tartrate C−H signal. The multicomponent complexes thus obtained were energy minimized, always keeping the geometry of βCD fixed as it was in the crystal structure.

Table 5—Intra- and Intermolecular Distances (Å) for the Proposed Complexes of the Two Enantiomers of *cis*-KC with βCD and TA, Represented in Figure 7, and Mean Values for the 12 Models Obtained after Rotation of the βCD around the Dichlorophenyl Ring, with Steps of 30°

	(+)-KC:TA:βCD		(–)-KC:TA:βCD	
	starting geometry	mean (range)	starting geometry	mean (range)
	Intramolecular Distances			
H20–H8	2.86	2.88 (2.47–3.15)	2.38	2.66 (2.38–3.20)
H20–H7	4.20	4.26 (3.99–4.52)	4.10	4.19 (3.95–4.59)
H5–H9′	3.32	3.24 (2.89–3.42)	3.09	3.18 (2.99–3.42)
H5–H9	2.79	3.07 (2.74–3.62)	3.30	3.27 (2.75–4.28)
	Intermolecular Distances			
H20–H3′βCD	2.39	2.48 (2.26–2.85)	2.22	2.46 (2.22–3.10)
H20–H5′βCD	3.04	3.22 (2.78–4.16)	3.07	3.36 (2.73–4.82)
H19–H3′βCD	3.47	3.55 (2.49–4.32)	3.73	3.29 (2.25–4.07)
H19–H5′βCD	2.50	2.52 (2.34–2.86)	2.70	2.52 (2.37–2.73)
H17–H3′βCD	2.41	2.51 (2.38–2.84)	2.34	2.54 (2.31–3.10)
H17–H5′βCD	2.64	2.50 (2.35–2.74)	2.64	2.70 (2.35–3.44)
H12/H13–H3′βCD[a]	3.81	3.81 (3.03–4.45)	3.74	4.01 (3.32–5.72)
H4–H3′βCD	2.94	3.24 (2.51–4.47)	2.65	3.31 (2.63–4.83)
H4–H2–H5′βCD[b]	4.32[c]	4.67 (4.23–5.07)	4.90[d]	4.91 (4.12–5.45)
H5–H3′βCD	2.63	2.86 (2.42–3.92)	2.44	2.95 (2.37–4.40)
H5–H2′/H5′βCD[b]	4.81[d]	4.66 (4.22–5.41)	4.27[c]	4.74 (4.27–6.75)

[a] The lower distance between H12–H3βCD and H13–H3βCD is reported, since the imidazole ring was not rotated (see Results and Discussion). [b] The H2′βCD and H5′βCD ^{1}H NMR signals were overlapped, and a unique assignment of NOE cross-peaks was impossible; the lower distances are reported. [c] With H2′βCD. [d] With H5′βCD.

Intermolecular distances were calculated in order to select those complexes which were consistent with the NOE cross-peaks observed. The cross-peaks were thus grouped on the basis of their intensity, each group corresponding to a different distance range: H17−H3′βCD and H17−H5′βCD were considered strong (protons closer than 2.5 Å) intensity peaks; H20−H3′βCD, H20−H5′βCD, H19−H5′βCD were considered medium (closer than 3.5 Å) intensity peaks; H19−H3′βCD, H4−H3′βCD, H4−H2′/H5′βCD, H5−H3′βCD, H12−H3′βCD, H13−H3′βCD were considered weak (closer than 5 Å) intensity peaks.[30] The intensity of H5−H2′/H5′βCD cross-peak cannot be assigned unambiguously, being overlapped with the H5−H9 intramolecular peak; therefore, distances lower than 5 Å were considered acceptable (vide supra).

Analysis of the intermolecular distances gave similar results for the two KC enantiomers, allowing the selection of a multicomponent complex, corresponding to KC conformer **3** in Table 4, which was in full agreement with NOE data; the intra- and intermolecular distances of the best multicomponent complex are reported in Table 5. The most significant difference between this complex and the other two, built up from conformer **1** and **2** of KC, concerns H20−H5′βCD distance: for the (−)-enantiomer this was 3.1 Å in the complex of conformer **3**, and 4.4 and 4.6 Å in the other two, while for the (+)-enantiomer it was 3.0, 4.4, and 5.7 Å respectively. These differences reflect the lower degree of inclusion of the dichlorophenyl ring into the βCD cavity in the two discarded models; in fact, the inclusion is partially forbidden by the position of the imidazole ring which "bumps" against the rim of βCD.

The βCD structure used for the docking studies is not symmetrical; to better explore the possible mutual orientations of the components of the complex, βCD was rotated, with 12 steps of 30° around the dichlorophenyl ring, keeping the ketoconazole tartrate fixed. Analysis of the intermolecular distances, after energy minimization, showed

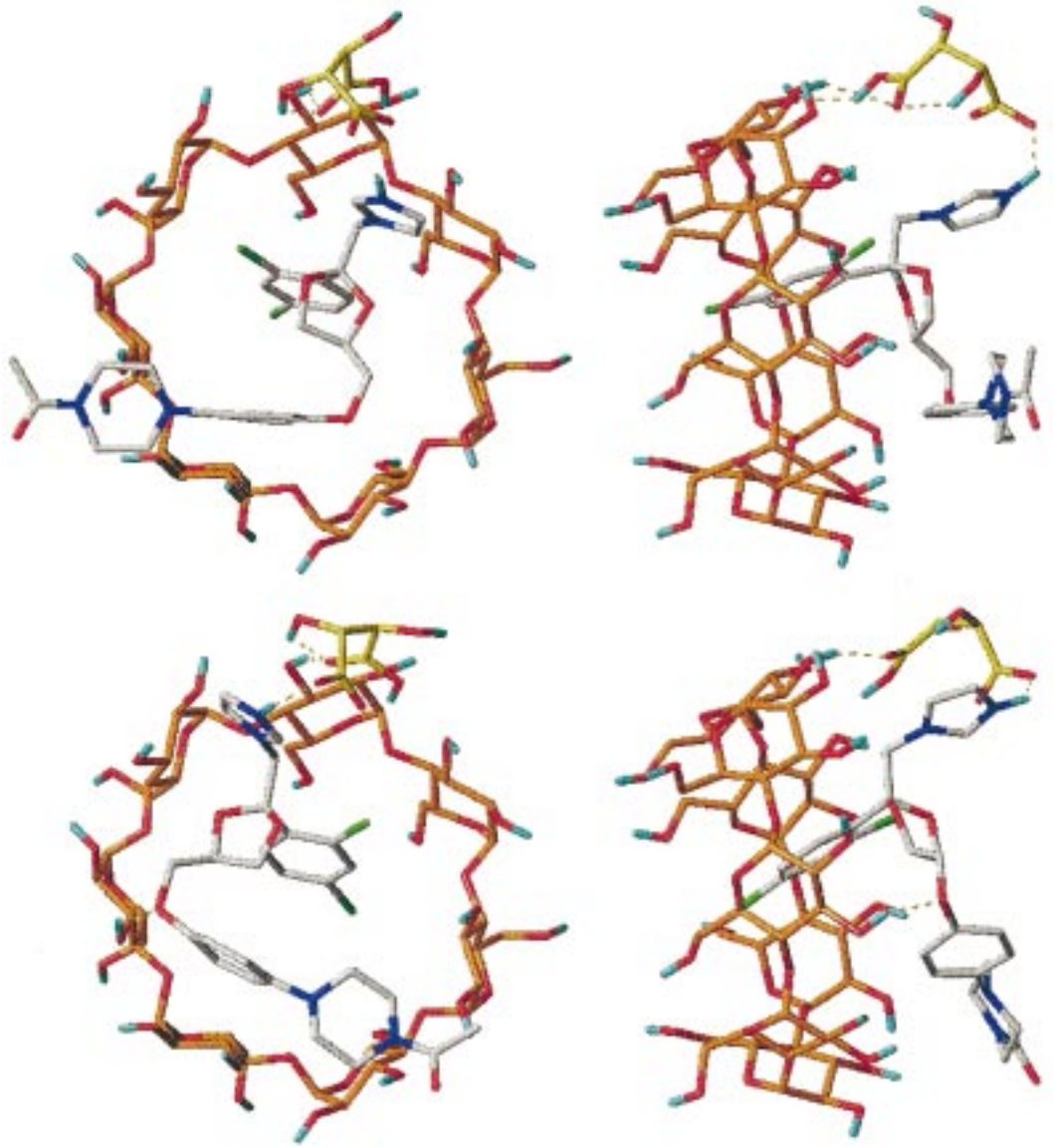

Figure 7—Representation of the multicomponent complex models for (+)- and (–)-KC (top and bottom, respectively) from the wider rim of βCD (left) and rotated by 90° on the *Y* axis (right); only polar hydrogens are displayed. Hydrogen bonds are indicated by dashed lines. Atom color codes – white: KC carbon; orange: βCD carbon; yellow: TA carbon; red: oxygen; blue: nitrogen; cyan: hydrogen; green: chlorine.

minor differences in some interatomic distances, compared to the starting geometry, but the mean values were still in agreement with the NOE cross-peak intensities, as reported in Table 5.

It has been stated that one of the major driving forces of drug−βCD complexation is a hydrophobic interaction between the guest molecule and the internal cavity of βCD.[31] Furthermore, the net entropy contribution was negligible in some cases,[28] but this fact could be attributed to the sum of entropy-favorable hydrophobic interaction and entropy loss due to conformational restriction. Under the hypothesis of similar entropy contribution for the two KC enantiomers, the interaction energy between the components, which is a rough estimate of the enthalpy contribution, can be regarded as an indication of different expected association constants. The interaction energy was therefore calculated for the multicomponent complexes of both the enantiomers of the selected KC conformation, to assess whether the higher association constant of the (−)-(2*S*,4*R*)-KC could be explained on the basis of tighter interactions. The energy values for the starting geometry of each complex, and the mean values calculated from the 12 models obtained after βCD rotation, are reported in Table 6. Comparison between the two enantiomers in terms of interaction energies can only be considered on a qualitative basis, being related only to the complementarity of the van der Waals surfaces (steric) and to the attractive and repulsive interactions between the assigned partial charges

Table 6—Interaction Energies (kcal/mol) between the Components of the Proposed Multicomponent Complexes for the Two Enantiomers of *cis*-KC. Energy Contributes for the Starting Geometry and Mean Values Obtained Rotating the βCD around the Dichlorophenyl Ring with Steps of 30° Are Reported

	(+)-KC:TA:βCD		(–)-KC:TA:βCD	
contribute[a]	starting geometry	mean ± SEM	starting geometry	mean ± SEM
El. KC:βCD	–2.19	–3.20 ± 0.42	–4.43	–3.48 ± 0.20
El. TA:βCD	–1.90	–1.29 ± 0.62	–3.74	–1.51 ± 0.55
El. KC:TA	–42.68	–41.76 ± 0.48	–42.10	–41.19 ± 0.42
St. KC:βCD	–20.80	–22.90 ± 0.72	–25.17	–23.30 ± 0.78
St. TA:βCD	–1.70	–2.13 ± 0.18	–2.15	–2.25 ± 0.13
St. KC:TA	0.79	0.33 ± 0.38	0.13	–0.15 ± 0.13
total	–68.48	–70.94 ± 1.17	–77.46	–71.89 ± 1.59

[a] El. = electrostatic energy; St. = steric energy.

(electrostatic). While significant differences in the interaction energies were observed for the starting geometry of the two complexes, they were much less pronounced, considering the mean values calculated for the 12 rotated models. However, the complex of the (−)-enantiomer was still characterized by a higher mean total interaction energy, although the small difference was comparable to the SEM of the data. This difference of about 1 kcal/mol, consistent with the small difference of association constant, was mainly due to the steric interaction between βCD and KC, but also to the electrostatic interaction of βCD with KC and TA, while the total (steric and electrostatic) interaction energy between KC and TA was approximately constant.

The starting geometry of the complexes formed by the two KC enantiomers are represented in Figure 7. As can be observed, besides the insertion of the dichlorophenyl ring into the internal βCD cavity, two additional interaction points are represented by the tartrate, bridging KC and βCD, and by the phenoxy fragment, located near the wider rim of βCD. Therefore, enantioselectivity results from the inclusion of an aromatic ring into the βCD cavity, the strong electrostatic interaction between the imidazolium tartrate moiety and βCD hydroxyl groups, and the accessory interaction of the phenoxy fragment with the wider rim of βCD, in agreement with the rule suggested by Armstrong.[31]

The real situation should be represented by an ensemble of different interconverting relative dispositions of the components of the complex; however, the reported model can be considered highly representative, as βCD seems to select some of the possible conformations of KC, as indicated by the H5−H9 and H5−H9′ intramolecular NOE cross-peaks. The different states of the complex include (i) the unexplored conformations of KC; in particular, those resulting from the rotation of the imidazole ring around C11−N bond could be related to enantioselectivity, as suggested by the different relaxation time variations of the imidazole protons for the two KC enantiomers; (ii) different orientations of the tartrate molecule with similar energy content, corresponding to each imidazole rotation; this multiplicity makes the arrangement of the imidazolium tartrate bridging region less defined, and, as a consequence, we considered H12 and H13 as equivalent in the calculation of the intermolecular distances; (iii) different possible relative orientations of KC and βCD, which we partially explored by rotation of the βCD; inclusion of other fragments into the βCD cavity could also occur at high CD concentrations, but the calculated lipophilicity profiles and the NMR data indicate that complex formation preferably occurs by inclusion of the dichlorophenyl moiety.

The Tripos force field put the piperazine ring of KC perpendicular to the benzene ring, while in the crystal structure they lie roughly on the same plane. Moreover, 24 different compounds containing a piperazinylphenyl substructure reported in CSD have the two rings almost in the same plane. The coplanar disposition of the two rings in our multicomponent complex could also be suggested by the presence of the very intensive H4−H2 NOE cross-peak; in fact, the distance between the two hydrogens is significantly lower in the coplanar disposition than in the perpendicular one. While our studies were conducted with the geometry resulting from energy minimization by the force field, repeated runs performed imposing the crystal geometry to the non-H atoms of the piperazinylphenyl fragment gave similar results in terms of intermolecular distances and chiral recognition.

Conclusions

An interaction model for both enantiomers of *cis*-KC with βCD in the presence of (+)-L-tartaric acid was built on the basis of preliminary ^{1}H NMR and ^{13}C NMR data. The measured intra- and intermolecular distances are in qualitative agreement with 2D NOE cross-peak intensities. This model, which probably represents the predominant solution structure, indicates that the inclusion of the dichlorophenyl moiety into the βCD cavity occurs from its wider-diameter side. Tartaric acid is strictly involved in the recognition process by establishing electrostatic interaction with the imidazolium ring and hydrogen bonds with 2- and/or 3-hydroxyl groups of βCD. A third interaction site is represented by the phenoxy fragment, involved in van der Waals and electrostatic interaction with the wider rim of βCD, with the possibility of hydrogen bond formation. These sites allow the definition of a chiral interaction; in fact, the association constants for the two KC enantiomers are slightly different, the (−)-one giving rise to the stronger interaction, in agreement with the calculated interaction energies for our models. The results are also consistent with patterns of chiral interactions proposed in the literature,[31,32] where the interactions with the 2- and 3- hydroxyl groups at the wider rim of CD appear to be the key element for the chiral recognition process.

References and Notes

1. Heeres, J.; Backx, L. J. J.; Mostmans, J. H.; Van Cutsem, J. Antimycotic Imidazoles. 4. Synthesis and Antifungal Activity of Ketoconazole, a New Potent Orally Active Broad Spectrum Antifungal Agent. *J. Med. Chem.* **1979**, *22*, 1003−1005.
2. Heel, R. C.; Brogden, R. N.; Carmine, A.; Morley, P. A.; Speight, T. M.; Avery, G. S. Ketoconazole: a Review of its Therapeutic Efficacy in Superficial and Systemic Fungal Infections. *Drugs* **1982**, *23*, 1−36.
3. Rotsein, D. M.; Ketesz, D. J.; Walker, K.; Swinney, D. C. Stereoisomers of Ketoconazole: Preparation and Biological Activity. *J. Med. Chem.* **1992**, *35*, 2818−2825.
4. Camps, P.; Farres, X.; Garcia, M. L.; Ginesta, J.; Pascual, J.; Mauleon, D.; Carganico, G. Stereoselective Syntheses of Both Enantiomers of Ketoconazole from (R)- and (S)-Epichlorohydrin. *Tetrahedron: Asymmetry* **1995**, *6*, 1283−1294.
5. Gray, N. M. WO 94 14447-A1, 1994.
6. König, W. A.; Gehrcke, B.; Hochmuth, D. H.; Mlynek, C.; Hopf, H. Resolution of Chiral [2.2]Paracyclophanes by Enantioselective Gas Chromatography. *Tetrahedron: Asymmetry* **1994**, *5*, 347−350.
7. Greatbanks, D.; Pickford, R. P. Cyclodextrins as Chiral Complexing Agents in Water, and their Application to Optical Purity. *Magn. Reson. Chem.* **1987**, *25*, 208−215.
8. Casy, A. F.; Mercer, A. D. Application of Cyclodextrins to Chiral Analysis by ^{1}H NMR Spectroscopy. *Magn. Reson. Chem.* **1988**, *26*, 765−774
9. Selva, A.; Redenti, E.; Pasini, M.; Ventura, P.; Casetta, B. A study of the salts with organic hydroxyacids of the Terfenadine β-Cyclodextrin inclusion complex in solution by Ionspray mass spectrometry. *J. Mass Spectrom.* **1995**, *30*, 219−220.
10. Vikmon, M.; Szemán, J.; Szejtli, J.; Pasini, M.; Redenti, E.; Ventura, P. In *Proceedings of the 7th International Cyclodextrins Symposium;* Osa, T., Ed.; Komiyama: Tokyo, 1994; pp 480−483.
11. Loftsson, T.; Brewster, M. Pharmaceutical Applications of Cyclodextrins. 1. Drug Solubilisation and Stabilization. *J. Pharm. Sci.* **1996**, *85*, 1017−1025.
12. Esclusa-Diaz, M. T.; Gayo-Otero, M.; Perez-Marcos, M. B.; Vila-Lato, J. L.; Torres-Labandeira, J. J. Preparation and Evaluation of Ketoconazole-β-cyclodextrin Multicomponent Complexes. *Int. J. Pharm.* **1996**, *142*, 183−187.
13. Gerloczy, A.; Szeman, J.; Csabai, K.; Kolbe, I.; Jicsinzky, L.; Acerbi, D.; Ventura, P.; Redenti, E.; Szejtli, J. Pharmacokinetic Study of Orally Administered Ketoconazole and its Multicomponent Complex on Rabbits of Normal and Low Gastric Acidity. In *Proceedings of the Eighth International Symposium on Cyclodextrins*; Szejtli, J., Szente, L., Eds.;

Kluwer Academic Publishers: Dordrecht, 1996; pp 515−518.
14. Part of the work was presented at the 9th International Symposium on Cyclodextrins, Santiago de Compostela, Spain, May 31−June 3, 1998.
15. Foster, R.; Fyfe, C. A. Interaction of Electron Acceptors with Bases. Part 15.-Determination of Association Constants of Organic Charge-Transfer Complexes by N. M. R. Spectroscopy. *Trans Faraday Soc.* **1965**, *61*, 1926−1631.
16. Benesi, B. H.; Hildebrand, J. H. A Spectrophotometric Investigation of the Interaction of Iodine with Aromatic Hydrocarbons. *J. Am. Chem. Soc.* **1949**, *71*, 2703−2707.
17. Powell, M. J. D. Restart Procedures for the Conjugate Gradient Method. *Mathematical Programming* **1977**, *12*, 241−254.
18. Peters, O. M.; Blaton, N. M.; De Ranter, C. J. *cis*-1-Acetyl-4-(4-{[2-(2,4-dichlorophenyl)-2-(1H-1-imidazolylmethyl)-1,3-dioxolan-4-yl]methoxy}phenyl)piperazine: Ketoconazole. A Crystal Structure with Disorder. *Acta Crystallogr., Sect. B* **1979**, *35*, 2461−2464.
19. Lindner, K.; Saenger, W. Topography of Cyclodextrin Complexes. Part XVII. Crystal and Molecular Structure of Cycloheptaamylose Dodecahydrate. *Carbohydr. Res.* **1982**, *99*, 103−115.
20. Heiden, W.; Goetze, T.; Brickmann, J. Fast Generation of Molecular Surfaces from 3D Data Fields with an Enhanced "Marching Cube" Algorithm. *J. Comput. Chem.* **1993**, *14*, 246−250.
21. Demarco, P. V.,; Thakkar, A. R. Cyclohepta-amylose Inclusion Complexes. A Proton Magnetic Resonance Study. *J. Chem. Soc., Chem. Commun.* **1970**, 2−4.
22. Djedaini, F.; Lin, S.; Perly, B.; Wouessidjewe, D. High-field Nuclear Magnetic Resonance Techniques for the Investigation of a β-Cyclodextrin: Indomethacin Inclusion Complex. *J. Pharm. Sci.* **1990**, *79*, 643−646.
23. Inoue, Y., NMR Studies of the Structure and Properties of Cyclodextrins and their Inclusion Complexes. *Ann. Rep. NMR Spectrosc.* **1993**, *27*, 59−101.
24. Breitmaier, E.; Voelter, W. *Carbon-13 NMR Spectroscopy;* VCH Publishers: New York, 1989; p 115 and p 259.
25. Haskins, N. J.; Saunders: M. R.; Camilleri, P. The Complexation and Chiral Selectivity of 2-Hydroxypropyl-β-cyclodextrin with Guest Molecules as Studied by Electrospray Mass Spectrometry. *Rapid. Comm. Mass Spectrom.* **1994**, *8*, 423−426.
26. Pocsfalvi, G.; Liptak, M.; Huszthy, P.; Bradshaw, J. S.; Izatt, R. M.; Vekey, K. Characterization of Chiral Host−guest Complexation in Fast Atom Bombardment Mass Spectrometry. *Anal. Chem.* **1996**, *68*, 792−795.
27. Selva, A.; Redenti, E.; Ventura, P.; Zanol, M.; Casetta, B. A Study of β-Cyclodextrin/Ketoconazole/tartaric acid Multicomponent Noncovalent Association by Positive and Negative Ionspray Mass Spectrometry. *J. Mass Spectrom.* **1998**, *33*, 729−734.
28. Lipkowitz, K, B. Applications of Computational Chemistry to the Study of Cyclodextrins. *Chem. Rev.* **1998**, *98*, 1829−1873 and references cited therein.
29. Lipkowitz, K. B. Symmetry Breaking in Cyclodextrins: a Molecular Mechanics Investigation. *J. Org. Chem.* **1991**, *56*, 6357−6367.
30. Neuhaus, D.; Williamson, M. *The Nuclear Overhauser Effect in Structural and Conformational Analysis*; VCH Publishers: New York, 1989.
31. Armstrong, D. W.; Ward, T. J.; Armstrong, R. D.; Beesley, T. E. Separation of Drug Stereoisomers by the Formation of β-Cyclodextrin Inclusion Complexes. *Science* **1986**, *232*, 1132−1135.
32. Lipkowitz, K. B.; Raghothama, S.; Yang J. Enantioselective Binding of Tryptophane by α-Cyclodextrin. *J. Am. Chem. Soc.* **1992**, *114*, 1554−1562.

Acknowledgments

The authors are grateful to Gabriele Amari and Giuseppe Pispisa (Chiesi Farmaceutici) for their experimental support. Financial support from the Italian MURST (40% and 60%) is gratefully acknowledged.

JS980468O